DSRII 771 PROD.TYPE: COM
pp. 1–21 (col.fig.: 1)
ED: SHIVA
PAGN: MVA – SCAN: MANGALA, PREETHY

PERGAMON

Deep-Sea Research II 00 (2000) 000–000

DEEP-SEA RESEARCH
PART II

Georges Bank Winds: 1975–1997

James Manning[a,*], Glenn Strout[b]

[a]*NOAA/NMFS, 166 Water Street, Woods Hole, MA 02543, USA*
[b]*Center for Marine and Scientific Technology, UMASS Dartmouth, MA 285 Old Westport Road, N. Dartmouth, MA 02747, USA*

Received 30 September 1998; received in revised form 6 January 2000

Abstract

Twenty-three years (1975–1997) of anemometer records from the four NOAA buoys located near Georges Bank are examined. While the individual buoy records have occasional gaps due to instrument breakdowns and the buoys deployments were limited to certain years, the combination of the four buoys provides a nearly continuous series of observed wind. After correcting for different anemometer heights, sea-surface wind stress is calculated by the neutral stability method of Large and Pond J. Phys. Ocean 11 (1981) 324. Weekly mean stress is plotted for the entire period. Significant coherence (0.72–0.92) was found between sites with very little phase or gain for the 2–10 day storm-band period. An offshore increase of ~ 0.006 Pa/100 km is detected in the mean stress for the Winter/Fall seasons. The complex correlation coefficients (calculated as a single measure of coherence across all frequency bands) ranges from 0.68 to 0.90. Other sources of wind data are discussed including the Fleet Numerical Meteorology and Oceanography Center's (FNMOC) estimates from pressure observations, the Comprehensive Ocean Atmosphere Data Set (COADS) from ship observations, and NOAA's National Center for Environmental Prediction (NCEP) recent model/data assimilation. For purposes of representing storm-band frequency, the FNMOC winds account for more than 80% of the variability in the buoy record and they provide a continuous surface wind estimate for the Georges Bank region back to 1967. However, the intensified wind stress as a function of distance offshore, as detected by both the buoys and COADS , is not detected in the FMNOC records. Also, a counterclockwise rotation of 19°_{max} is needed (in addition to the standard 15°) to correct the FMNOC winds for the atmospheric boundary layer. Recent NCEP products provide a finer scale spatial coverage of the wind field and are a potential source of boundary forcing for coastal ocean circulation models.

* Corresponding author. Fax: + 1-508-495-2258.
E-mail address: jmanning@whsun1.wh.whoi.edu (J. Manning).

0967-0645/00/$ - see front matter
PII: S0967-0645(00)00116-8

1. Introduction

Wind forcing of ocean circulation on Georges Bank (Brink, 1983; Noble et al., 1985; Manning and Beardsley, 1996) is significant enough that frequent storm events may have important consequences to annual recruitment and survival of pelagic fish eggs and larvae (Werner et al., 1993; Lough et al., 1994; Landsteiner et al., 1996; Lewis et al., 2000). Since wind forcing contributes substantially to surface dynamics, an understanding of the persistent and aberrant features of wind is fundamental for modeling the dynamics of Georges Bank. Since ocean circulation models are now formulated to investigate a variety of processes ranging from interannual to storm-band scales, it is necessary to examine these same periods in the wind variability. With this as a primary motivation, an attempt is made here to summarize the nearby NOAA buoy anemometer records to date and supplement these observations with other sources of wind information.

The objective is to determine the character of the wind field on Georges Bank. Of particular interest are the major forms of spatial and temporal variability. Have there been significant year-to-year differences in wind? Is the wind field spatially coherent across Georges Bank? Can model-generated wind products be used as reliable estimates of the wind field and are they consistent? These are questions that arise in preparation of ocean circulation modeling/hindcasting. In order to exercise the regional models now under development for this area, it is first necessary to document the properties of this primary forcing mechanism that drives the current field.

Though several estimates of mean wind stress on Georges Bank have been reported in the literature, there are inconsistencies. These inconsistencies are attributable to differences in the raw data, the algorithms used to average wind speed and direction, the frequency band considered, and the methods used to calculate the wind stress. As an example, in Table 7.1 of Hopkins and Raman's review (1987) several estimates of monthly mean wind stress are listed for the Georges Bank region. The values for March and April, the biologically important months, vary by more than an order-of-magnitude. Most of these estimates and others from the literature (Saunders, 1977; Godshall et al., 1995) are derived from ship observations. Due to the numerous terms needed to formulate wind stress, different methods for parameterizing the wind stress were used. Harrison (1989) generated monthly mean wind-stress estimates for the world's ocean in 1° squares from over a century of ship observations and found a 20–30% reduction in wind stress relative to those of Hellerman and Rosenstein (1983), which he attributed to formulation of the drag coefficient. Hellerman and Rosenstein, in comparing their estimates to earlier works of others, attributed differences to having used a different portion of the COADS input data and having used different smoothing procedures on the output data. In this report, records from relatively stable buoy platforms are used to generate indices of wind on the sea surface. The difficulties involved with these estimates are discussed and other sources of wind information that are available today are compared to the buoy records.

With more than two decades of anemometer records from the NOAA buoys and more than three decades of modelled wind now available, the interannual, seasonal, and storm–related frequencies can be examined. As discussed in Hopkins and Raman (1987), Georges Bank is exposed to a variety of synoptic weather systems. The origin, track, and frequency of these systems vary seasonally, which complicates the analysis of variability in the wind stress. The region is affected by both cyclones and anticyclones but is dominated by the former. The cyclones form due to various cold

outbreaks along the jet stream and warm fronts of older mature cyclones. Systems pass Georges Bank approximately once per week (more frequently in the winter months) and have residence times of 1–2 days.

2. Moored buoy data

Regular wind observations in the vicinity of Georges Bank began when the first lightship was moored on Nantucket shoals on 15 June 1854. Less than a year later, a strong wind blew it off station and onto the beach at Montauk, New York (Flint, 1989; Thompson, 1983). So began a long history of the most exposed moored lightship in the world, the Nantucket Lightship (NTLS). After being blown off station 29 more times in severe weather and more than a dozen replacement vessels (some sank), the final NTLS was discontinued on 20 December 1983. It was the last US lightship.

The digitized records of NTLS wind were obtained for the period 1975–1982. In 1982, the manned lightship was replaced with one of NOAA's automated Large Navigational Buoys (LNB) identified as 44008 (see Fig. 1), resulting in a change in anemometer height from roughly 17 to 13.8 m. The anemometer height was reduced to 5 m in May 1996 when it became a discus buoy. Meanwhile, buoy 44003 had been positioned on the southeast side of Great South Channel since 1978. Its anemometer remained constant at 5 m above the waterline until the buoy was discontinued in 1984. Buoy 44011, the most seaward of the four buoys discussed here, is located two-thirds the way across the southern flank of Georges bank. It underwent a change in anemometer height from 10 to 5 m in March of 1985. Buoy 44005, located in the Gulf of Maine, had changed its anemometer

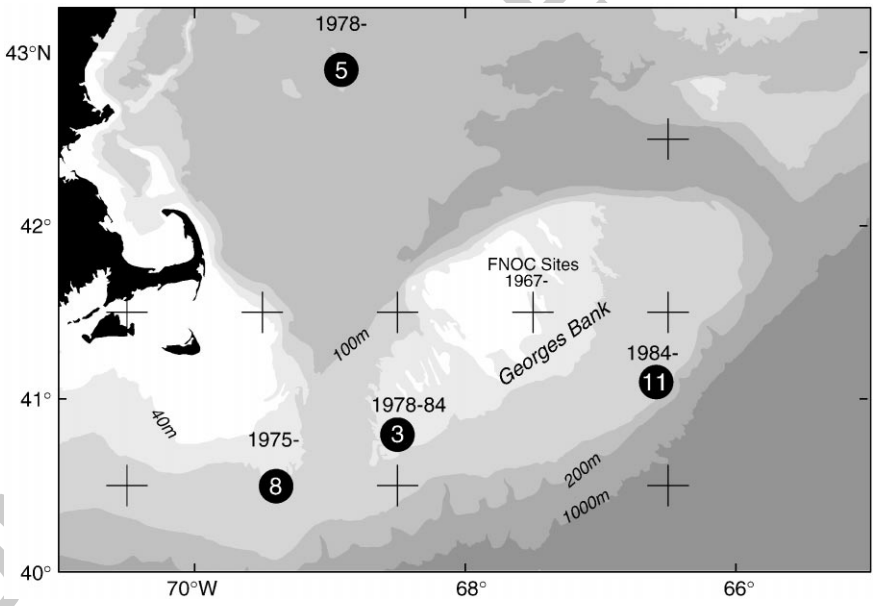

Fig. 1. Geographic location of NOAA buoys (circles) and FNMOC grid sites (crosses). Bathymetry is shaded and labeled. Buoy "8", for example, refers to buoy 44008.

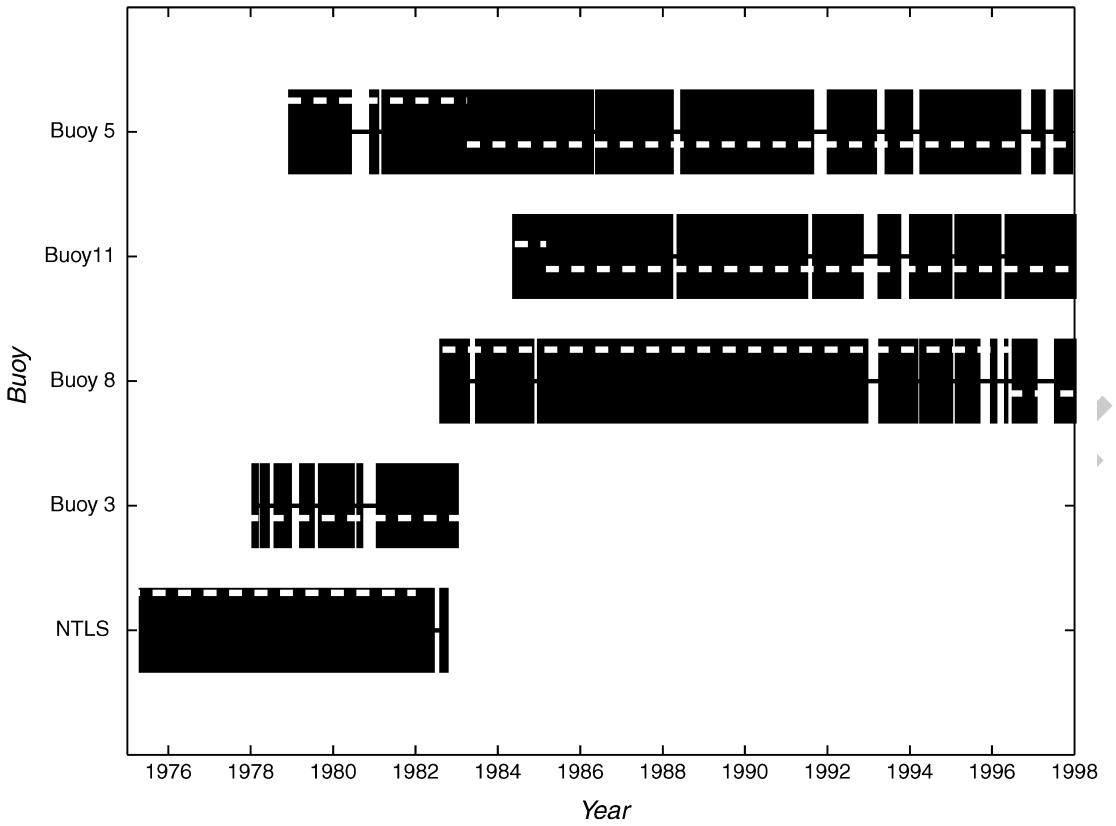

Fig. 2. Periods of good wind data (1975–1997) on Georges Bank. Dashed lines represent relative anemometer heights ranging from 5 to 17 m.

height (13.8–5 m) in April of 1983. It also changed position (55 km) in April 1994, which resulted in a water depth change (200–29 m). Fig. 2 depicts the data record used in this report and the relative anemometer heights. Table 1 outlines the operating periods and hardware of the NOAA buoys. (Only those sensors that provided data for this report are listed. Many of the NOAA buoys have a variety of sensors not discussed here. Much of the information and data from the National Data Buoy Center are available at http://seaboard.ndbc.noaa.gov including information on their anemometers calibration and correction for local magnetic variation.) For details pertaining to the components and accuracy (± 1 m/s for speed and 10° for direction) of NOAA buoys refer to Gilhousen (1987) and Gilhousen (1988). Air and sea temperatures from the buoys were used to assess the effects of air–sea thermal stability on wind.

3. Other sources of wind data

The Comprehensive Ocean Atmosphere DataSet (COADS, Slutz et al., 1985) was acquired on CD-ROM from the Pacific Fisheries Environmental Group (PFEG, NMFS, Monterey, CA). The

Table 1
Buoy deployment periods, sensor configuration, and geographic location

Buoy no.	Period	Sensor		Height (m)	Water depth[a] (m)	Position
		Anemometer		5.0		
44003	3/77–4/84	Air temp.		4.0	53	40.8 N 68.5 W
		Sea temp.		− 1.0		
		Anemometer	< 1Apr'83	13.8	200	< 1Apr'94 42.7 N 68.3 W
			> 1Apr'83	5.0		
44005	12/78–12/97	Air temp.	< 1Apr'83	11.4	29	> 1Apr'94 42.9 N 68.9 W
			> 1Apr'83	4.0		
		Sea temp.		− 1.0		
		Anemometer	< 1May'96	13.8		
			> 1May'96	5.0		
44008	8/82–12/97	Air temp.	< 1May'96	11.4	63	40.5N 69.4W
			> 1May'96	4.0		
		Sea temp.	< 1May'96	− 1.1		
			> 1May'96	0.6		
		Anemometer	< 1Mar'85	10.0		
			> 1Mar'85	5.0		
44011	5/84–12/97	Air temp.	< 1Mar'85	10.0	88	41.1 N 66.6 W
			> 1Mar'85	5.0		
		Sea temp.		−1.0		

[a]Water depth of station.

data contained release 1 for years 1854–1980 and the Interim release for years 1980–1990. Data were extracted as monthly means in 1° geographic bins using the CODE routine (Mendelssohn and Roy, 1996). Lightships and buoys were excluded from the data selection. Anemometer heights are unknown. All data (no trimming) from the period 1960–1990 were used in the analysis.

The US Navy's Fleet Numerical Meteorology and Oceanography Center (FNMOC, formerly FNOC, Monterey, California) has conducted Sea-Level Pressure Analysis (SLPA) of the North American continent and surrounding oceans for more than three decades. While the amount of input data and their analysis techniques have changed over time, they estimate geostrophic wind fields from the sea-level pressure output. The PFEG's Aromark program makes such an estimate of wind for user-specified locations. The Aromark program uses as many as 16 grid points from the original 63×63 FNMOC grid to make an estimate at each specified point. These estimates (Bakun, 1973), sometimes referred to as "Bakun Winds", are smoothed over time as well because the original SLPA incorporate some climatology and persistence at data-limited time steps. Hence, while nine grid points (1°) on Georges Bank were acquired (denoted by crosses (+) in Fig. 1), the data are not spatially and temporally independent samples.

The National Environmental Predictions Center (NCEP, formerly NMC), a branch of NOAA's National Weather Service (NWS), has been generating and archiving their data assimilated forecast every 6 h since 1990 (Black, 1994; Rogers et al., 1996). They have gradually increased the number of grid points to a resolution of approximately $\frac{1}{4}$ degree and have focused on the sub-synoptic structure with some models now outputting 3-h forecasts. Their model is spun up with their Eta Data Assimilation System (EDAS) for 12 h prior to the forecast run. Their forecast run, known as their mesoscale "Eta Model", is examined below.

4. Methods

A series of processing steps were conducted on the buoy records prior to the calculation of wind stress. Depending on the payload of instrumentation, National Data Buoy Center (NDBC) processed the raw 8.5-min samples through to hourly averages by either the "vector" or "scalar" method. The former method was used on the older General Service Buoy payload and the later used on the Data Acquisition, Control, and Telemetry payload. While the difference in the two processing methods is reported as minimal ($< 7\%$, Gilhousen, 1987), direct comparisons (coherence and phase) of buoy records using different payloads were avoided in this report. The hourly averaged wind speed as received from NDBC was converted from knots to meters/second when necessary. The time series of the east/west and north/south components were then cleaned of spikes by replacing each point outside of two standard deviations in a 10-h running mean by the mean of that 10 h. The resulting time series was then spline fit to an evenly spaced 3-h time series, and holes greater than 3 h were designated as missing values. The spline fit was then compared to the original 10-h running means to eliminate spurious peaks that the spline fits had introduced. This resulting time series is therefore a set of observations filtered for investigating storm periods that are typically at least several hours duration, and higher-frequency processes were eliminated from the analysis.

In order to estimate stress, the method of Large and Pond (1981) was employed. As it has been used extensively in the literature in the last decade

$$\tau_{\text{buoy}} = \rho C_{\text{d}} |U| U, \tag{1}$$

where $C_{\text{d}} = 0.0012$ for $U < 11$ m/s, and $C_{\text{d}} = (0.49 + 0.065|U|) \times 10^{-3}$ for $U > 11$ m/s, where ρ is the density of air (1.25 kg/m^3) and $|U|$ is the estimate of wind speed at 10 m above the sea surface. Estimates are corrected for anemometer height by assuming a log–layer boundary (Ruggles, 1970). We have assumed neutral stability (i.e. no stratification in the atmospheric boundary layer).

In this study, a relative measure of wind stress is obtained in order to depict anomalous events. The complexity of the atmospheric bottom boundary layer is recognized, but the calculation of stress, as described above, ignores many of the secondary processes. While an accurate measure of the sea-surface stress is important in studies of the air–sea interface and heat flux, the qualitative estimates of stress reported here may be thought of as an indices of wind-driven advection rather than an absolute measure of stress.

For example, there is often a thermal gradient at the air–sea boundary, but we treat the effect on stress as insignificant. Stability corrections are sometimes applied (Smith, 1988) to account for the variation in drag due to the air–sea temperature difference, but corrections were not applied to this

dataset since the thermal gradient information was not available for much of the study period (1975–1997). For a selected period in 1992, however, a sensitivity test was conducted to investigate this effect of stability. Using the formulation in Large and Pond (1981), the Monin–Obukov length and Richardson number were calculated. The 10 m wind speed was then adjusted due to stability. Except for the instances where the stratification was high and the absolute wind speed were low, most corrections were minimal. The largest difference was in January and February when the air temperature was typically more than 3° colder than the sea-surface temperature. Differences in stress values resulting from this correction in the monthly -mean sense were minimal ($< 3.3\%$).

Since there are several months of overlapping time series (Fig. 2) from the various sites, coherence, phase, and gain could be calculated among sites as a function of frequency and season. Since the overlap between buoy time series is less than a few months in some cases, frequency bands of a few weeks or less were examined in order to obtain at least 20 degrees of freedom. Averaging over at least three frequency bands was conducted in order to obtain results of $> 95\%$ confidence. These calculations were done for various combinations of the east/west and north/south components of wind stress. Rotary spectra (Gonella, 1972) for both cyclonic and anti-cyclonic rotations of complex wind stress vectors were conducted, as well. In addition to the frequency-dependent spectral results, the complex correlation coefficient (Kundu, 1976), phase, and transfer function was calculated as a measure of the overall relationship between sites.

In the calculation of weekly and monthly means for a particular buoy, any periods when the number of observations in that period was less than half of the maximum number possible were eliminated from further analysis. Given 3-h records, this cutoff corresponds to $N_{\min} = 28$ and $N_{\min} = 120$ for weekly and monthly means, respectively.

In the calculation of mean annual cycle for the whole bank area, a combination of monthly means were used. In other words, for each month of the entire period (1975–1997) at least one buoy was in operation so that a monthly mean file was generated with each month represented by one buoy. For months where more than one buoy was operating, a single buoy was chosen as representative. For example, buoy 44008 was chosen over buoy 44005 because its proximity to Georges Bank. The composite mean monthly mean was then generated from this file. A file of weekly means (1975–1997) was also generated with representative buoys.

In the case of the COADS data, since the individual observations were not accessible, the "monthly mean pseudo-stress" was extracted from the database. To generate an estimate of stress, the equation

$$\tau_{\mathrm{COADS}_j} = \rho C_{\mathrm{d}} \frac{\sum U_j^2}{N} \tag{2}$$

was used where U_j is the component of wind velocity, N is the total observations being considered for the particular month, C_{d} is the drag coefficient (0.00126), and ρ is the density of air (1.25). The number N, which varies greatly bin-to-bin and year-to-year, often translates to less than one observation per day especially for those grids on the offshore (eastern) side of Georges Bank. Other monthly mean wind stress estimates from the literature (Hellerman and Rosenstein, 1983; Harrison, 1989; Saunders, 1977) also were obtained to compare with those calculated directly from the COADS data.

In the case of FNMOC data, a measure of "psuedo–stress" at the seasurface is provided as 19.5 m geostrophic wind that has been rotated counter-clockwise 15° to account for Ekman veering, reduced by 30% to account for atmospheric boundary layer friction, and then subjected to the formula as in Eq. (1) with drag coefficients as described for Eq. (2).

In the case of the NCEP modeled winds, a set of forecast files was downloaded each day from their ftp server. For each of the 6-h files from 6 to 36 h, the 10 m winds were extracted from the forecast fields for comparison with buoy winds. Since the model nodes did not fall exactly on the buoy sites, a linear interpolation was made of the modeled winds at the buoy sites.

5. Results

The observed weekly mean wind stress is plotted in Fig. 3a and b for the first and second half of the record, respectively. Except for a few weeks in some years, the entire period is covered by at least one of the four NOAA anemometers in the vicinity of Georges Bank. The strong winds of January through April are generally out of the north–northwest followed by lower and more variable winds in May/June, steady winds from the southwest in July/August, and then a highly variable transition back to winter winds (Fig. 4).

As noted in Table 3 (rows 9 and 10), the FNMOC modeled wind stress is fairly coherent with the nearby NOAA buoys especially for periods greater than 2 days. More than 80% (coherence = 0.89 and 0.81) of the low-frequency wind stress variability is captured by the modeled fields at the buoy sites 44008 and 44011. The observed wind stress is relatively lighter and stronger (gains 0.92 and 1.12) than the nearby FNMOC sites for lower-frequency bands, but the phase differences are not significantly different from zero. As discussed in Pazan et al. (1982) and described in more detail below, the FNMOC products are generated with interpolation over time and space. Therefore, they are expected to produce a smoothed, "blended", and lower-frequency time series than the observational records.

5.1. Time variability

The degree of inter-annual variability is most easily depicted in the form of progressive vectors in Fig. 5. This record from the FNMOC site on the southern flank of Georges Bank indicates that, while there is a general eastward trajectory of the air mass, there are periods in the late winters of 1967, 69, 73, and 87: for example, when there were anomalous episodes of flow towards the west and south. However, the principal axis of variability for particular months is, in general, aligned with the axis of mean wind.

Since each of the buoys provide several years of data and since most of each year (1975–1997) had at least one operating buoy, a composite mean monthly mean and mean standard deviations was made for the entire period (Table 2). The standard deviations are nearly an order of magnitude greater than the mean.

5.2. Spatial variability

In the comparison of simultaneous time series (for a nine-month period in 1990 when three buoys 44005, 44008, and 44011 were operating consistently), significant coherence between buoys

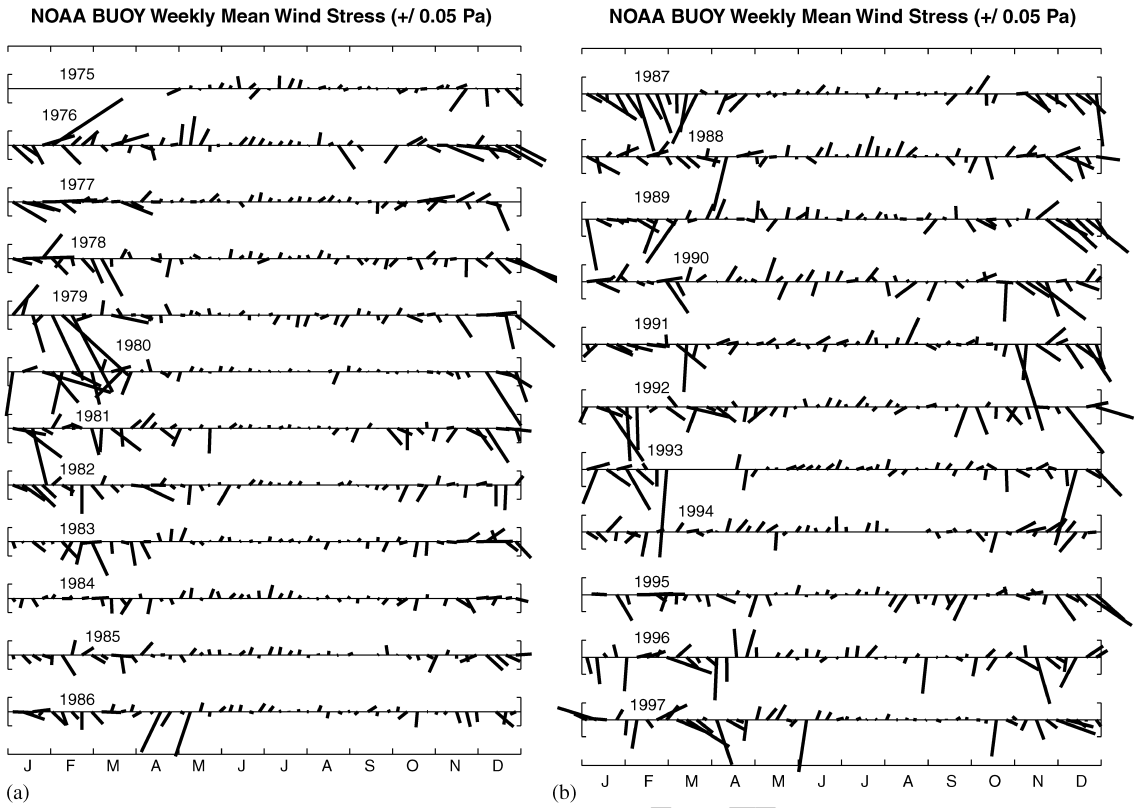

Fig. 3. (a) Stickplot of weekly-mean wind stress at NOAA buoys: 1975–1986. *Y*-axis brackets represent the 0.05 Pa scale; (b) Stickplot of weekly mean wind stress at NOAA buoys: 1987–1997. *Y*-axis brackets represent the 0.05 Pa scale.

(Fig. 6) was found with little difference in amplitude and phase. The agreements fall off as expected in the higher-frequency bands and become insignificant for periods less than approximately 1 day. The most coherent relationship in Table 3 was between buoys 44008 and 44003 since these buoys were located in the same vicinity. NTLS and buoy 44008 were even closer together, but their overlap time was limited and the method and frequency of observations was not the same so that a good comparison is difficult. In Table 3, the frequencies of highest coherence for various overlapping time periods are listed with the 95% confidence level in parenthesis. Results indicate that the wind field around Georges Bank is statistically coherent (0.72–0.92) at synoptic time scales. The gains between all sites ranged from 0.57 to 1.22. The lowest (0.56) gain, from NTLS to buoy 44003, and the highest (1.22) gain, from the NTLS to buoy 44008, likely are artifacts of the lightship data as discussed below. In addition to the frequency-dependent results, the "complex correlation coefficient" is listed along with the corresponding phase and gain in the last three columns of Table 3. These results are similar to the coherence of highest significance and the phases are again near zero. An example two-month time series of three buoys, as well as FNMOC @41N67W, is given in Fig. 7, which depicts the coherence in a visual form and demonstrates the lack of higher-frequency variance missing from the FNMOC record.

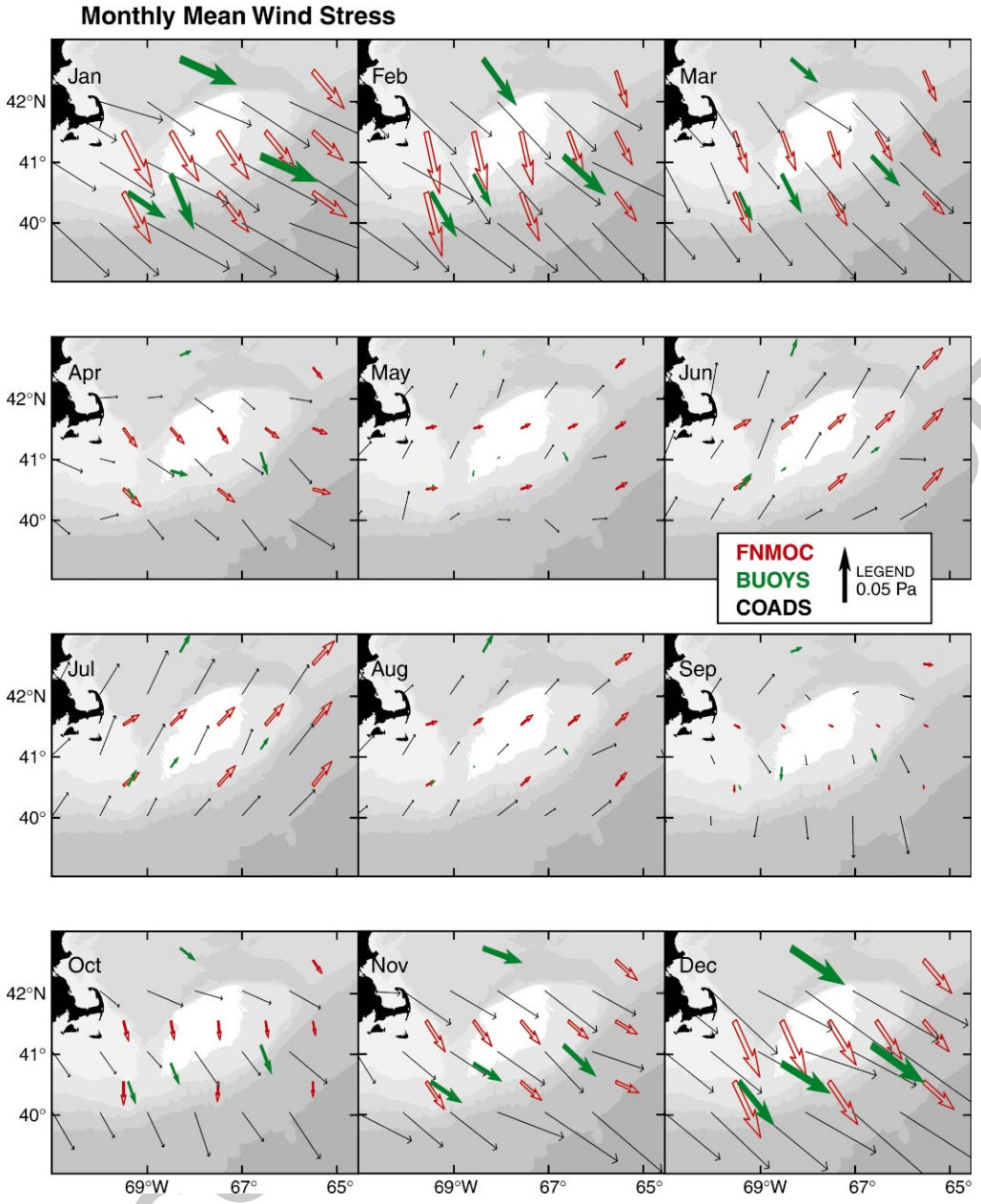

Fig. 4. Monthly mean wind stress vectors for four NOAA buoy locations (44003, 44005, 44008, and 440011, solid arrows), FNMOC sites (hollow arrows), and COADS bins (this arrows). The legend is shown in the lower right corner of the September panel. The bathymetry level of < 60 m (white), 100, 200, and > 1000 m depths are shaded to depict the Georges Bank outline.

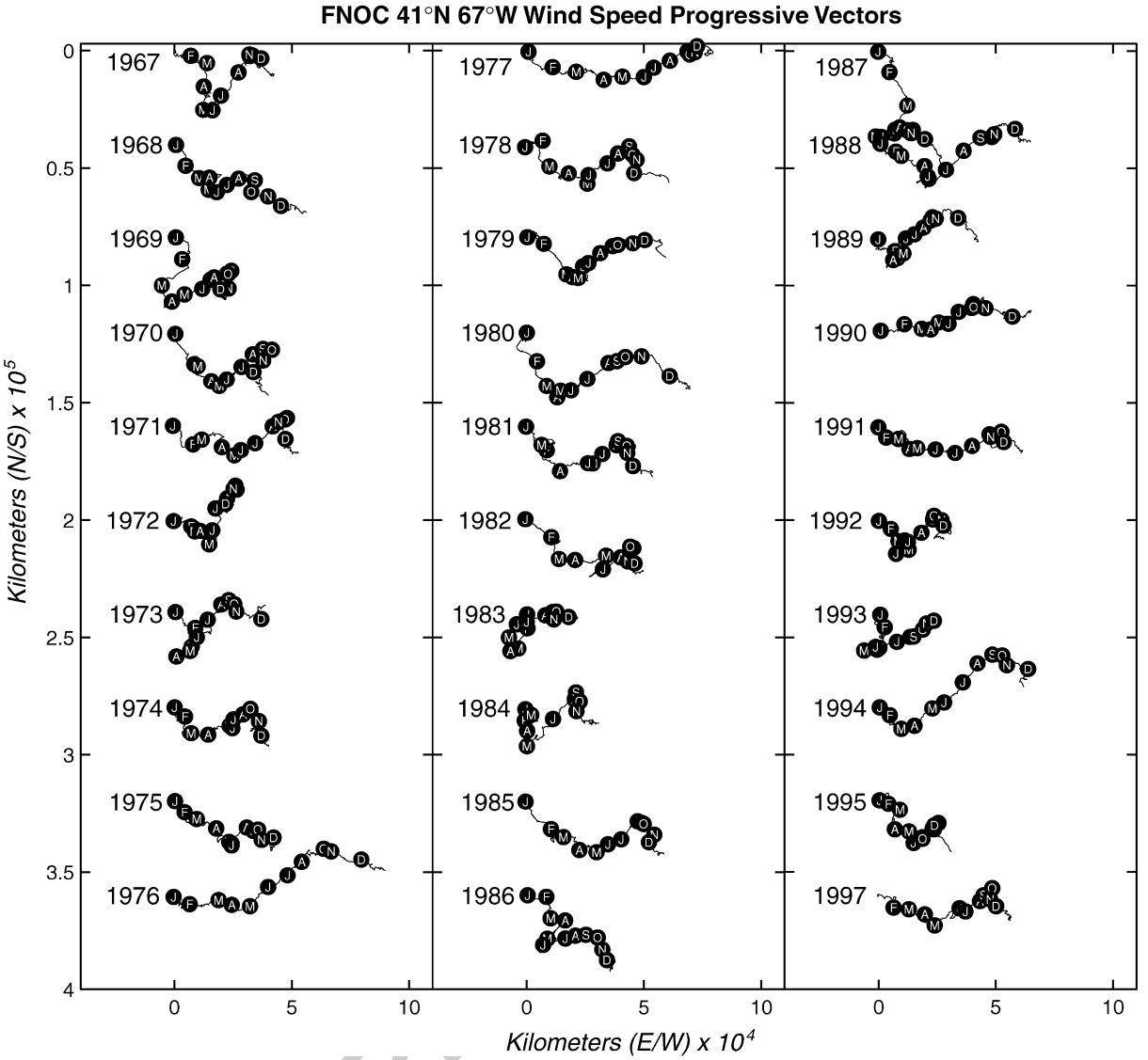

Fig. 5. Progressive vector diagram of the FNMOC wind on the southern flank of Georges Bank indicating the cumulative effect of each 6-h estimate spanning the entire three decades 1967–1997 (1996 missing). The beginning of each month is indicated by a labeled black circle. Successive years are offset by 40000 km on the *y*-axis.

In order to examine the spatial variability in the wind stress field, all data sources were used. The change, if any, of the wind stress magnitude as a function of longitude was the focus of this investigation. Is there a significant difference in the wind stress in the vicinity of the Great South Channel (near buoy 44008) relative to the eastern flank of Georges Bank (near buoy 44011)? The answer depends on the frequency, the time of year, and the component of wind stress under investigation. While the scalar mean wind stress is often stronger off-shore, the vector mean stress

Table 2
Monthly mean wind stress statistics (1975–1997)

Month	Eastward stress				Northward stress				Resultant[a]	
	Mean[b] (Pa)	Std[b]	Min[b]	Max[b]	Mean[b]	Std[b]	Min[b]	Max[b]	Dir[b] (to)	Magnitude[b] (Pa)
1	0.055	0.145	− 0.41	0.82	− 0.023	0.116	− 0.63	0.44	112	0.060
2	0.036	0.137	− 0.41	0.65	− 0.029	0.120	− 0.70	0.38	129	0.047
3	0.035	0.124	− 0.42	0.56	− 0.021	0.107	− 0.44	0.39	121	0.041
4	0.013	0.088	− 0.33	0.37	− 0.009	0.089	− 0.41	0.29	124	0.016
5	0.004	0.049	− 0.18	0.17	0.002	0.069	− 0.27	0.38	65	0.004
6	0.009	0.038	− 0.14	0.13	0.010	0.045	− 0.18	0.17	44	0.014
7	0.008	0.030	− 0.16	0.14	0.014	0.034	− 0.13	0.14	30	0.016
8	0.005	0.048	− 0.21	0.31	0.003	0.054	− 0.36	0.20	59	0.006
9	0.002	0.052	− 0.18	0.25	− 0.007	0.065	− 0.33	0.25	162	0.007
10	0.013	0.090	− 0.34	0.41	− 0.018	0.087	− 0.44	0.28	144	0.022
11	0.040	0.116	− 0.34	0.53	− 0.019	0.102	− 0.49	0.30	116	0.044
12	0.054	0.144	− 0.44	0.64	− 0.043	0.127	− 0.58	0.37	129	0.069

[a]Vector average of taux and tauy.
[b]Means values over all years. The values listed for "min", for example, are the mean minimum for those months and not the absolute minimum over the entire 23 yr.

may be lower in some months of some years. This would result from the wind being lighter but more *consistent* in direction nearer the coast. As noted in the fifth entry in Table 3, coherence in the storm band ($\sim$ 3 days) is 0.84. The gain function indicates a decrease (0.76) offshore in this frequency band. However, when the analysis is redone to include only the Fall of 1990 (6th entry in Table 3), a gain of greater than 1.0 for the most significant frequency band results. It should be noted, though, that the gain function is not an ideal measure of amplitude changes since (a) it is really only meaningful with high coherences, and (b) it applies to changes in the variability rather than the mean values. It may be impossible, therefore, to resolve a frequency-dependent spatial relationship of two buoy sites from such short overlap periods.

To investigate this spatial variability in more detail it is necessary to examine records of multiple decades. The FNMOC records at grid points along the 40 and 41°N (last two entries in Table 3) were examined first. The storm-band gain is near unity (> 0.93). However, in the month-band frequency (see hollow arrows in Fig. 4), the relationship changes with season. While the FNMOC summer southwesterlies apparently increase offshore (see June–August in Fig. 4), the winter wind stress (December–February) evidently does not. This result does not hold up, however, for the case of COADS and buoy data where estimates of longitudinal variation along the 41°N (Table 4) indicate the opposite: a significant wintertime increase of stress in the offshore sites.

In order to further examine the *seasonal variation* in the spatial relationship, a continuous time series at buoy 44008 and 44011 was generated by filling missing values with FNMOC 41N70W and 41N66W, respectively, for the entire period 1984–1994. The complex correlation functions were calculated for each month and a mean taken over all years. The results indicate a decrease in the

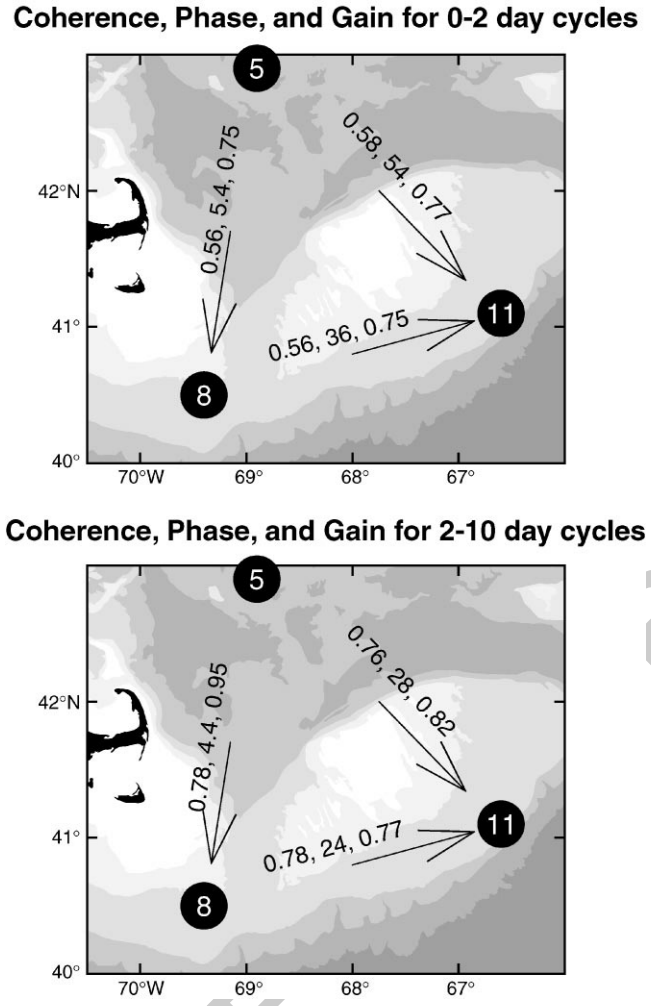

Fig. 6. Cross-spectral relationship between buoys 44005, 44008, and 44011 including values of coherence, phase (deg), and gain for both the (a) 0–2 day cycles and (b) 2–10 day cycles. Results are averaged over multiple frequency bands (see Table 3 for specific frequencies). Negative phase angle implies first record leads the second.

correlation coefficient during the summer without any obvious seasonal pattern in gain or phase. The spatially -smoothed FNMOC winds, however, may introduce a bias to this process. They fail to capture the longitudinal variation in monthly mean stress that appear in both the shipboard and buoy observations.

Another process that confounds the offshore variation in wind stress is the rotational aspect of the wind stress. When the decade-long series of buoys 44008 and 44011 were subjected to rotary spectra analysis, the storm-band coherence is stronger for anti-cyclonic component. This likely results from the anti-cyclones being in the form of a front. They move in a relatively straight path with consistent rotation at all sites. The cyclonic weather systems, on the other hand, generate variation in rotation depending on the track of the storm relative to the buoy site.

Table 3
Coherence, phase, and gain between sites and overall complex correlation coefficient

Buoy pair	Time period	# days	Separation (km)	Period[a] (day)	Coherence (Sig)	Phase[b] (CI)	Gain	Deg. of freedom	Complex correlation	Phase[b]	Gain
NTLS-44008	19Aug–26Sep'82	39	~ 0	2.1	0.80 (0.33)	9 (11)	0.85	27	0.62	8	0.48
NTLS-44003	11Mar'81–31Dec'81	295	83	5.0	0.82 (0.30)	4 (10)	0.57	34	0.83	− 4	0.57
NTLS-44005	01Jan–17Apr'79	107	261	2.5	0.72 (0.35)	− 2 (16)	1.22	24	0.62	5	0.61
44008–44003	18Aug–21Dec'82	125	83	3.3	0.92 (0.37)	− 3 (8)	1.00	21	0.90	4	0.89
44008–44011	31Mar–31Dec'90	276	245	2.9	0.84 (0.35)	− 19 (12)	0.76	24	0.75	− 6	0.69
44008–44011	1Sep–31Dec'90	123	245	8.1	0.78(0.37)	− 9 (14)	1.04	21	0.76	− 7	0.70
44005–44011	31Mar–31Dec'90	276	227	2.9	0.83 (0.35)	− 24 (12)	0.79	24	0.72	− 5	0.68
44005–44008	31Mar–31Dec'90	276	261	2.9	0.85 (0.35)	6 (10)	0.96	24	0.80	4	0.82
44008-FNMOC	31Mar–31Dec'90	276	145	2.9	0.89 (0.35)	0 (8)	0.92	24	0.86	16	0.76
44011-FNMOC	31Mar–31Dec'90	276	67	2.3	0.81 (0.35)	− 18 (12)	1.12	24	0.80	13	0.78
40 N 70 W–66 W	01Jan–31Dec'90	365	354	2.4	0.82 (0.38)	− 56 (13)	0.94	20	0.74	− 7	0.82
41 N 70 W–66 W	01Jan–31Dec'90	365	334	2.4	0.86 (0.38)	− 59 (11)	0.95	20	0.73	− 6	0.80

[a] Period of maximum coherence.
[b] Positve phase indicates the second series leads the first series.

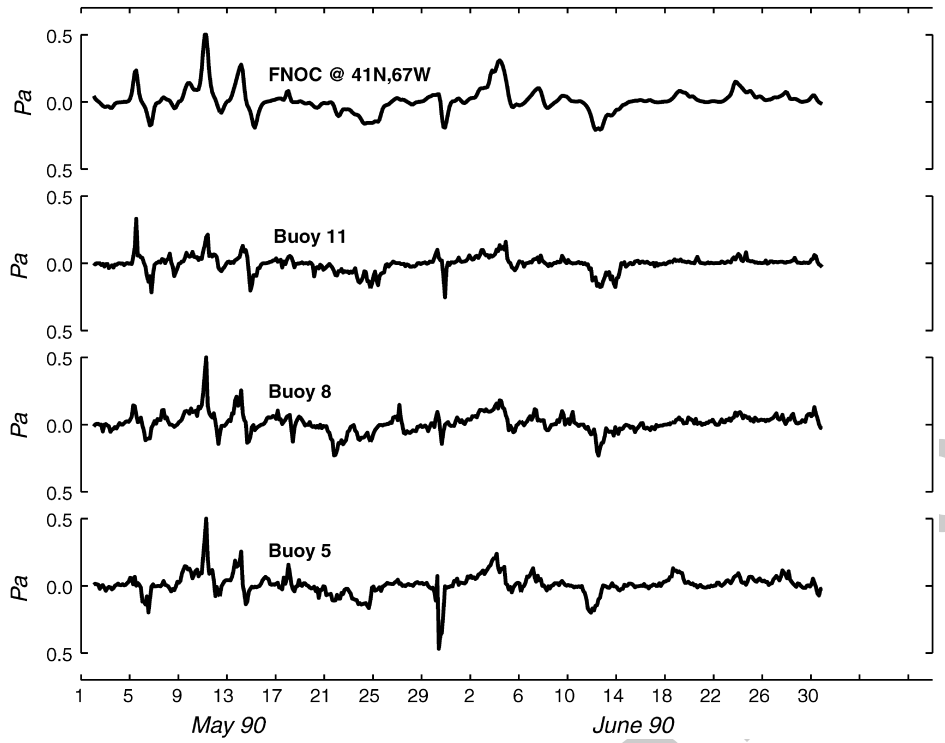

Fig. 7. Example time series of northward wind at three NOAA buoys and FNMOC wind records (May–June 1990).

In conclusion, the *variation* of spatial relationships with data source, frequency band, season, year, and rotational direction is likely larger than the *mean* spatial relationship, but the direct observations by buoys and ships indicate a significant increase of 0.006 Pa/100 km for the winter/fall periods.

6. Discussion

As noted above, the gain factors from one buoy to another may be artifacts of the stress calculation. In the case of buoy 44008 and 44011, for example, winds are recorded at 13.8 and 5 m, respectively. While a log–layer correction was applied to the wind speed to adjust the magnitude to 10 m, there are undoubtedly other factors in the non–linear processes of the atmospheric boundary layer that are not considered in this analysis. Ruggles (1970) for example, showed a series of irregularities in the wind profile over the ocean that occur at different wind speeds and sea state (roughness). He suggested that the drag coefficient is closely tied to surface wave development stages and that there is a peak, for example, at the transition between capillary and gravity wave generation ($\sim$ 4 m/s wind). Large and Pond (1981) noted that, when one is interested in periods less than a day or so, the drag coefficients should be adjusted lower or higher depending on whether the wind is increasing or decreasing. Given the size of the weather systems on Georges Bank, it may often be the case that the wind is increasing at one site and decreasing on the other.

Table 4
Estimates of longitudinal variation in wind stress.

Data	Season	longitude range	Pa/100 km	Correlation coefficient
Buoy 8–11	Annual	69–66 W	0.003	NA
	Winter		0.007	NA
	Spring		0.002	NA
	Summer		− 0.001	NA
	Fall		0.005	NA
Buoy 3–11	Annual	68–66 W	0.005	NA
COADS @40 N	Annual	71–65 W	0.004	0.41
	Winter		0.011	0.90
	Spring		0.009	0.81
	Summer		0.004	0.29
	Fall		0.005	0.71
FNOC @41	Annual	70–66 W	0.000	0.07
H&R @41[a]	Annual	71–67 W by 2	0.009	0.91
	Winter		0.019	0.99
	Spring		0.014	0.88
	Summer		0.003	0.89
	Fall		0.008	0.91
Harrison @41[b]	Annual	70.5–65.5 W	0.003	0.47
	Winter		0.002	0.39
	Spring		0.004	0.61
	Summer		0.001	0.30
	Fall		0.006	0.56
Saunders @40.5[c]	Annual	70.5–66.5 W	0.009	0.90
	Winter		0.009	0.88
	Spring		0.007	0.94
	Summer		0.003	0.88
	Fall		0.003	0.87

[a]Hellerman and Rosenstein (1983).
[b]Harrison (1989).
[c]Saunders (1977).

6.1. FNMOC vs. buoy winds

The overall monthly means (Fig. 4) indicate that the standard 15° rotation of FNMOC model winds may not be enough to correct for Ekman veering. In the case of the buoy 44008 comparison, where the FNMOC grid node falls nearest the vicinity of the direct measurement, an additional 19°counter-clockwise rotation is needed to correct the FNMOC wind stress direction. For other areas of the bank the annual mean correction is equal or less than this amount and tends to be most needed in the winter months. Hence, the 26° "veering" of wind on Georges Bank suggested by Hopkins and Raman (1987) may be partly due to their use of FNMOC winds on the offshore side of the bank. Another indication that the FNMOC product requires additional rotation is found in

the phase calculation of the complex-correlation coefficient, which accounts for all frequency bands. As listed in Table 3, comparisons with buoy 44008 and 44011 indicated phase shifts of 16° and 13°, respectively, relative to the FNMOC time series. This result indicates that the FNMOC winds may not have captured the intensity of the steady winter winds from the west. The general conclusion, therefore, is that the correction may be as large as 19° in a monthly mean sense and near zero for storm band frequencies. This conclusion supports that of DeYoung and Tang (1989) who showed the direction adjustment may be greater for lower wind speeds. Directional adjustment also was reported by Thomson (1983) who suggested the FNMOC winds are 20° to the right of those measured on buoys off the British Columbian coast, by Luick et al. (1987) who indicated an additional 44° is needed off the Gulf of Alaska, and by Halliwell and Allen (1984) who suggested additional rotations based on a location off the California coast. FNMOC's 30% reduction factor appears to be adequate in general, but this amplitude adjustment may depend on exact location, season, and, of course, on the method used to estimate stress from buoy winds. Note that FNMOC does not adjust their "psuedo–stress" drag coefficient (0.00126) as a function of wind stress.

6.2. Spatial variability

Are there detectable differences in the character of the wind on Nantucket Shoals (buoy 8) relative to the offshore (buoy 11)? The influence of individual storms and the dependence on storm tracks through a particular region (as shown by the NCEP example below) may govern estimates of spatial gradients in wind stress for relatively short-time series. Three decades of FNMOC records (1967–1997), however, should be long enough. They indicate a subtle increase off-shore during the summer months of the vector average stress and a decrease off-shore during the remainder of the year (see Fig. 4). Comparison of buoy 44008 vs. buoy 44011 did not depict this relationship in a monthly mean sense, and their spectral relationship in the storm-band varies with season and year. The monthly means of the buoy series (1984–1997) still may be highly influenced by individual storms, and a relationship of this type is hard to distinquish from the noise, but the fact that buoy estimates agree with this COADS analysis, as well as other COADS analyses in the literature, indicates that the buoy records are more accurate. The variation in the spatial relationship with season is not as clearly defined for Georges Bank as it may be in other areas such as the Southern Atlantic Bight (Wiesberg and Pietrafesa, 1983), but, as documented in Table 4, the general result is an increase in wind stress offshore for most months. Independent analyses of longterm COADS data (Hellerman and Rosenstein, 1983; Harrison, 1989; Saunders, 1977) support this conclusion.

Many of today's ocean circulation models use assimilated winds provided by government agencies such as the NCEP. As an example of the spatial coverage and resolution that is available today, Fig. 8 presents a snapshot of a single storm (Hurricane Eduoard, see Williams et al., 2000) in September 1996. This example demonstrates the potential differences in wind direction that may occur when a large cyclone passes directly over Georges Bank. Note the difference in wind direction at buoy 44008 vs. buoy 44011. A more typical weather pattern resulting from fronts passing through the region on a near-weekly basis, while not as dramatic as the cyclone shown, often produces sharp variations in the wind field vectors. The output of this early eta weather model compares well with buoy observations in the Georges Bank region (Fig. 9). For an in-depth comparison of other weather model surface parameters, see Baumgartner and Anderson (1999).

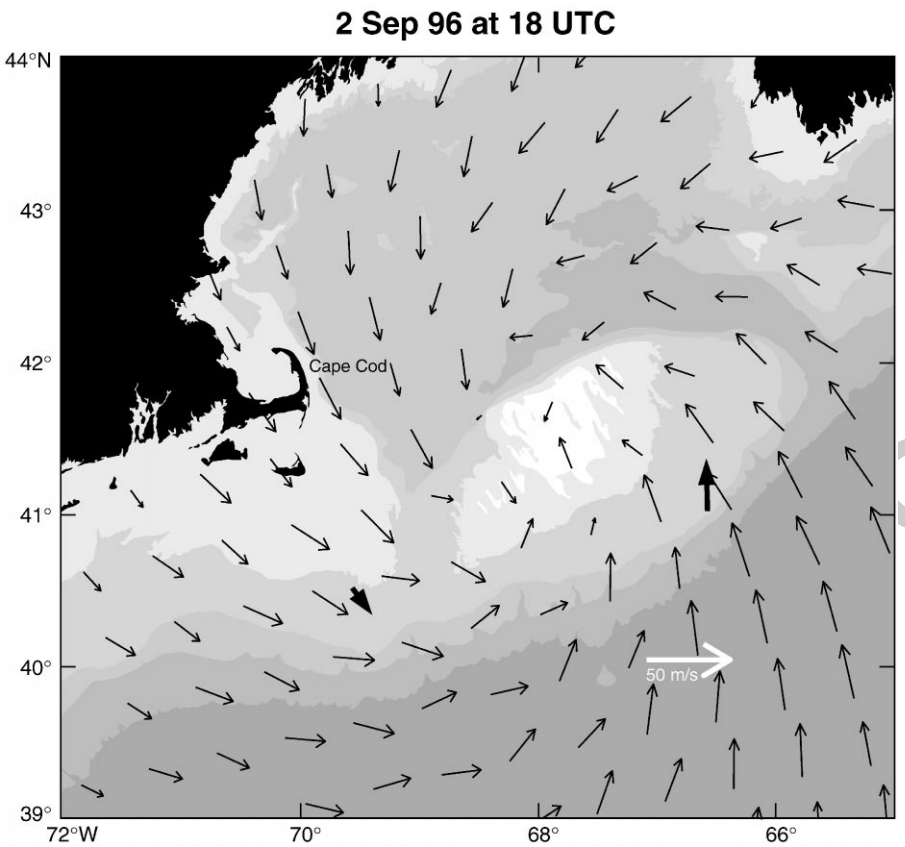

Fig. 8. An example of the data-assimilated wind field as generated by NOAA/NCEP eta- model using a combination of observations and modeling. The parameter plotted here is their estimated wind from the 40 km resolution grid at 10 m above the sea surface. The example depicts the passage of Hurricane Eduoard (see Williams et al., this issue). Buoy observations are plotted with thick arrows at 44008 and 44011.

7. Summary

Wind records from NOAA buoys in the vicinity of Georges Bank were adjusted for anemometer height, and a relative measure of stress was calculated by the method of Large and Pond (1981). The entire time series is presented graphically in a variety of forms to depict the general features of the wind field. Aside from a large seasonal cycle, the dominant variability is contained in the 2–10 day storm -band and is fairly coherent (0.72–0.92) across the bank, especially for the anti-cyclonic rotations. The principal axis of variability is generally aligned with the monthly mean stress. Given this high coherence, small phase changes ($\pm$ 20°), and small amplitude changes (gains 0.76–1.04) between buoys, each series may be considered representative of the entire region, such that a nearly continuous record is available for the period of 1975–1997.

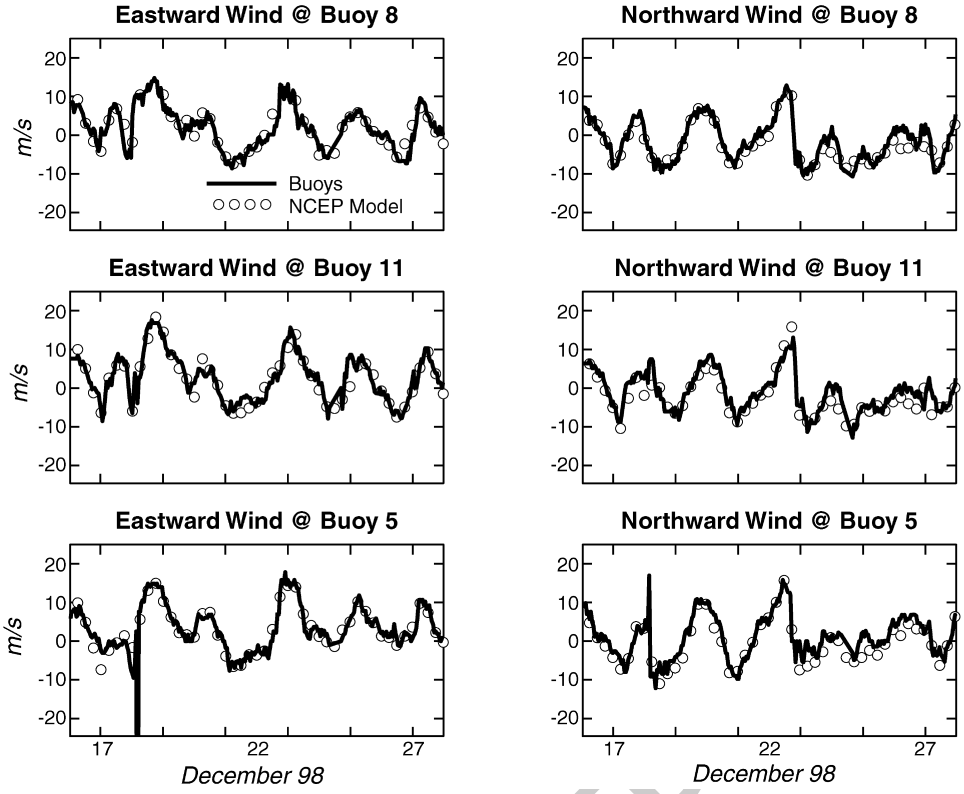

Fig. 9. Comparison of NCEP's daily eta model 3–36 h forecast wind and buoy observations.

Cross-spectral quantities between buoys vary significantly with frequency so that a single spatial relationship cannot be concluded. Spectral analysis of buoy records for particular seasons of particular years is likely biased by a few strong storm events. Unlike the monthly and seasonal mean fields, the synoptic fields do contain significant spatial structure. This storm-induced structure can be easily detected in recent NWS/NCEP regional model output.

The FNMOC modeled winds are accurate estimates of the low–frequency (2–10 day) winds on Georges Bank. However, as demonstrated in other regions off the coast of the United States, the FNMOC modeled winds on Georges Bank need an additional counter-clockwise rotation to portray accurately the seasonally averaged stress ($\leqslant 19^{\circ}$). This extra rotation is evidently most needed during periods of low winds. The FNMOC winds do not capture the spatial variability that is detected in the more direct observations on buoys and ships. Making quantitative estimates of wind stress with the COADS shipboard data on Georges Bank is not easy given the irregularity of the data over time and space, the uncertainty of the anemometer heights, and the limited access to raw data, but the general conclusions of seasonal and spatial variability tend to agree with the buoy data.

8. Uncited Reference

Butman and Beardsley 1987.

Acknowledgements

The authors thank the modeling team, Drs. Lynch (Dartmouth Col.), Loder (Bedford Institute of Oceanography), and Lough (NMFS) for the initial encouragement and support; D. Mountain and R. Signell for multiple reviews; D. Gilhausen (NDBC) for granting our requests and answering our questions; C. Lewis for debugging processed buoy data; Roy Mendelssohn and Jerry Norton (PFEG) for providing ship and model wind data, respectively; and E. Kleindinst and D. Hiltz for maintaining our computer network. This project was funded by the US GLOBEC: Importance of Physical and Biological Processes to Population Regulation of Cod and Haddock in Georges Bank; A Model-Based Study. US GLOBEC Contribution XXXX.

References

Bakun, A., 1973. Coastal upwelling indices, West Coast of North America 1946–1971. NOAA-TR-NMFS-SSRF 671, pp. 1–12.

Baumgartner, M.F., Anderson, S.P., 1999. Evaluation of NCEP regional numerical prediction model surface fields over the Middle Atlantic Bight. Journal of Geophysical Research 104 (C8), 18141–18158.

Black, T.L., 1994. The new NMC Mesoscale Eta model: description and forecast examples. Weather and Forecasting: NMC Notes 9, 265–278.

Brink, K.H., 1983. Low-frequency free wave and wind-driven motions over a submarine bank. Journal of Physical Oceanography 13, 103–116.

Butman, B., Beardsley,R.C., 1987. Long-term observations on southern flank of Georges Bank. Journal of Physical Oceanography 367–384.

DeYoung, B., Tang, C.L., 1989. Analysis of FNOC winds of the Grand Banks. Atmosphere-Oceanography 2, 414–427.

Flint, W., 1989. Lightships of the United States Government. A bicentennial Publication of the U.S. Coast Guard Historian's Office, Washington, D.C.

Gilhousen, D.B., 1987. A field evaluation of NDBC Moored Buoy winds. Journal of Atmospheric and Oceanic Technology 4, 94–104.

Gilhousen, D.B., 1988. Quality Control of Meteorological Data from Automated Marine Stations. Fourth International Conference on Interactive Information and Processing Systems for Meteorology, Oceanography and Hydrology, Anaheim, CA. Amer. Meteor. Soc., Boston, MA, pp. 248–253.

Godshall, F.A., Walker, H.A., Cayula, S.C., 1995. Scales of coastal wind variability by COADS wind summaries in 2° square areas. In: Diaz, H.F., Isemer, H-J. (Eds.), Proceedings of the International COADS Winds Workshop, Kiel Germany, 31 May-2 June 1994. NOAA Environmental Research Lab.

Halliwell, G.R., Allen, J.S., 1984. Large-scale sea level response to atmospheric forcing along the west coast of North America, Summer 1973. Journal of Physical Oceanography 14, 864–886.

Harrison, D.E., 1989. On climatological monthly mean wind stress and wind stress curl fields over the world ocean. Journal of Climate 2, 57–70.

Hellerman, S., Rosenstein, M., 1983. Normal monthly wind stress over the world ocean with error estimates. Journal of Physical Oceanography 13, 1093–1104.

Hopkins, T.S., Raman, S., 1987. Atmospheric variables and patterns. In: Backus, R.H., Bourne, D.W. (Eds.), Georges Bank. MIT Press, Cambridge, MA, 593 pp.

Kundu, P.K., 1976. Ekman Veering observed near the ocean bottom. Journal of Physical Oceanography 6, 238–242.

Landsteiner, M.C., Bollens, S.M., Davis, C.S., Solow, A.R., Green, J.R., Manning, J.P., 1996. The effects of storm events on the distribution and abundance of zooplankton on Georges Bank: 1939–1987. EOS. Abstract for AGU Spring Meeting 1996.

Large, W.G., Pond, S., 1981. Open ocean momentum flux measurements in moderate to strong winds. Journal of Physical Oceanography 11, 324–336.

Lough, R.G., Smith, W.G., Werner, F.E., Loder, J.W., Page, F.H., Hannah, C.G., Naimie, C.E., Perry, R.I., Sinclair, M., Lynch, D.R., 1994. Influence of wind-driven advection on interannual variability in cod egg and larval distribution on Georges Bank: 1982 vs. 1985. ICES Marine Science Symposium, Vol. 198, pp. 356–378.

Luick, J.L., Royer, T.C., Johnson, W.R., 1987. Coastal atmospheric forcing in the NorthernGulf of Alaska. Journal of Geophysical Research 92 (C4), 3841–3848.

Manning, J.P., Beardsley, R.C., 1996. Assessment of Georges Bank recirculation from Eulerian current observations in the Great South Channel. Deep-Sea Research II 43 (7–8), 1575–1600.

Mendelssohn, R., Roy, C., 1996. Comprehensive Ocean Dataset Extraction-User's Guide. NOAA Tech. Mem. NMFS-SWFSC-228, LaJolla, CA, 65pp.

Noble, M., Butman, B., Wimbush, M., 1985. Wind-current coupling on the southern flank of Georges Bank: variation with season and frequency. Journal of Physical Oceanography 15, 604–620.

Pazan, S.E., Barnett, T.P., Tubbs, A.M., Halpern, D., 1982. Comparison of observed and model wind velocities, 1982. Journal of Applied Meteorology 21, 314–320.

Rogers, E., Black, T.L., Deaven, D.G., DiMego, G.J., Zhao, Q., Baldwin, M., Junker, N., Lin, Y., 1996. Weather and Forecasting: NMC Notes 11, 391–413.

Ruggles, K.W., 1970. The vertical mean wind profile over the ocean for light to moderate winds. Journal of Applied Meteorology 10, 389–395.

Saunders, P., 1977. Wind Stress on the ocean over the eastern continental shelf of North America. Journal of Physical Oceanography 7, 555–566.

Slutz, R.J., Lubker, S.J., Hiscox, S.D., Woodruff, S.D., Jenne, R.L., Joseph, D.H., Steurer, P.M., Elms, J.D., 1985. Comprehensive Ocean-Atmosphere Data Set; Release 1. NOAA Environmental Res. Lab., Climate Res. Program., Boulder, CO., 268pp.

Smith, S.D., 1988. Coefficients for sea surface wind stress, heat flux and wind profiles as a function of wind speed and temperature. Journal of Geophysical Research 93 (C12), 15467–15472.

Thompson, F.L., 1983. The Lightships of Cape Cod. Congress Square Press. Portland, ME.

Thomson, R.E., 1983. Comparison between computed and measured winds. Journal of Geophysical Research 88 (C4), 2675–2683.

Werner, F.E., Page, F.E., Lynch, D.R., Loder, J.W., Lough, R.G., Perry, R.I., Greenberg, D.A., Sinclair, M.M., 1993. Influences of mean advection and simple behavior on the distribution of Cod and Haddock early life stages on Georges Bank. Fisheries Oceanography 2 (2), 43–64.

Wiesberg, R.H., Pietrafesa, L.J., 1983. Kinematics and correlation of the surface wind field in the South Atlantic Bight. Journal of Geophysical Research 88 (C8), 4593–4610.